





Article

Evaluation of Satellite Precipitation Products for Hydrological Modeling in the Brazilian Cerrado Biome

Jhones da S. Amorim ^{*}, Marcelo R. Viola , Rubens Junqueira , Vinicius A. de Oliveira  and Carlos R. de Mello

Department of Water Resources and Sanitation, Federal University of Lavras, Lavras 37200-900, Brazil; marcelo.viola@ufla.br (M.R.V.); rubensjunqueira@live.com (R.J.); aovinius@gmail.com (V.A.d.O.); crmello@ufla.br (C.R.d.M.)

* Correspondence: jhonesamorim@gmail.com; Tel.: +55-35-3829-1684

Received: 28 July 2020; Accepted: 12 September 2020; Published: 15 September 2020



Abstract: This study investigates the applicability of Satellite Precipitation Products (SPPs) in streamflow simulations performed in the Brazilian Cerrado biome, which is one of the world's biodiversity hotspots. Local data from ground observations were used as a reference for evaluating the Tropical Rainfall Measuring Mission (TRMM) Multi-satellite Precipitation Analysis (TMPA) and Integrated Multi-Satellite Retrievals for Global Precipitation Measurement (IMERG). The Soil and Water Assessment Tool (SWAT) was used to simulate the streamflow in a subbasin of the Tocantins river basin. Statistical precision metrics showed that both SPPs presented a satisfactory performance for precipitation monitoring on a monthly scale, in which IMERG performed better than TMPA. The Nash–Sutcliffe coefficient and Kling–Gupta efficiency obtained for both calibration and validation period were greater than 0.82 and 0.79, respectively, demonstrating that both SPPs were able to simulate the hydrological regime adequately. However, the bias indicated that the SPPs overestimated the observed streamflow. The r-factor and p-factor values showed that both TMPA and IMERG presented low uncertainty in streamflow simulations. SPPs offer a great alternative for monitoring the precipitation and hydrological studies in the Brazilian Cerrado biome, and presented better simulation results than rain gauges.

Keywords: GPM IMERG; TRMM-TMPA; Soil and Water Assessment Tool; Brazilian Savana

1. Introduction

Precipitation is one of the main components of the hydrological cycle due to the significant role that it plays in various socio-economic activities. It involves complex physical processes and displays high spatial and temporal variability [1–3]. Accurate estimates of precipitation are crucial for a wide range of climate and hydrology applications [4]. Despite its importance, in several locations around the world, the monitoring network of precipitation has limitations related to density, frequency of observations, and infrastructure [2].

The rain gauges provide data for calibration and validation for other precipitation data sources [5]. They are considered the reference data source for precipitation [3] and the most adequate data for hydrological modeling. However, rain gauge measurements have limitations, such as spatial coverage and point measurement, mainly in tropical developing regions, where high variability makes precipitation one of the most difficult weather variables for estimating [1]. Furthermore, only a few countries can afford a dense rainfall monitoring network [6]. Currently, Brazil has an average density of one rain gauge per 720 km² [7], which is below that recommended by the World Meteorological

Organization. Moreover, precipitation regimes of large areas in Brazil are not recorded due to the uneven spatial distribution of rain gauges [6].

Despite providing data with a high spatial and temporal resolution, ground-based radar systems are not feasible in developing countries due to the high cost and maintenance required [8]. To overcome these limitations, Satellite Precipitation Products (SPPs) are a promising alternative to improve spatial precipitation measurements [9,10]. In recent decades, SPPs have been available with nearly global coverage and high space-time resolution [3,10], such as the Tropical Rainfall Measurement Mission Multi-satellite Precipitation Analysis (TMPA) [11] and Integrated Multi-satellite Retrievals for Global Precipitation Measurement (IMERG) [12].

TMPA was the first dedicated meteorological precipitation satellite to be used worldwide [1,8,9,13–17]. However, Gadelha et al. [7] have highlighted a need to assess the accuracy of TMPA in comparison to ground-based data on a regional basis. After the Tropical Rainfall Measurement Mission (TRMM), IMERG was launched to provide the next generation of multi-sensor precipitation data more accurately, since the Ka-band in the Dual-frequency Precipitation Radar (DPR) used by Global Precipitation Measurement (GPM) is more sensitive than the TRMM Precipitation Radar (PR) in light rainfall [4]. Studies assessing the performance of IMERG for precipitation estimation have been carried out in different regions of the world [18–20]. A recent study to evaluate the applicability of IMERG in Brazil was performed by Gadelha et al. [7]. Nevertheless, they did not use IMERG version 6 (launched in June 2019), which introduces significant improvements over to the previous version [12].

Since the accuracy of SPPs varies with the characteristics of the region and season of the year [17,21–23], and streamflow simulations are profoundly affected by the uncertainties associated with precipitation datasets [1], recent studies have used the propagation of the precipitation errors in hydrological simulations to evaluate the reliability of SPPs [6,8,10,18,24].

Bitew and Gebremichael [25] stated that the use of the SPPs as inputs in hydrological models has two main advantages. The first is the reduction of the spatial variability that arises using rain gauges directly to validate the SPPs, since the models are performed at a basin scale. The second is the validation of the SPPs for a specific application, which is typical in water resource planning, instead of just precipitation monitoring. In addition, SPPs can overcome the limitations that arise from the low densities of rain gauge networks and provide a better representation of the spatial variability of precipitation, therefore improving the hydrologic model performances [8,26].

The Brazilian Cerrado biome covers approximately two million square kilometers of the central area of the country [27] and is the second-largest biome in South America. Also referred to as the Brazilian Savanna, the Cerrado is one of the richest and most endemic biomes of the world [28] and has suffered severe anthropogenic impacts such as agricultural expansion and livestock activities [29]. For this reason, the Cerrado is considered one of the environmental hotspots of the world [30].

The Cerrado biome plays an essential role in the water supply and social-economic development of Brazil since it is present in the headwaters of major basins in Brazil and South America such as the Paraná, Paraguai, Tocantins, and São Francisco [31]. Furthermore, a significant portion of the Gurani aquifer, one of the largest aquifer systems of the world and the largest reservoir of groundwater in South America, is located in the Cerrado [31,32]. Nobrega et al. [29] stated that the water balance components in the Cerrado are poorly understood and their hydrological characterization is often limited. Thus, understanding the hydrological dynamics in the Cerrado biome is crucial for water management in Brazil and South America.

Given that SPPs are a possible alternative for hydrological modeling, and the importance of the Brazilian Cerrado biome to biodiversity and water supply, the objectives of this study were to: (i) assess the reliability of TMPA and IMERG precipitation products concerning conventional ground-based measurements (rain gauges) in a basin located in the Cerrado biome; (ii) calibrate and validate the Soil and Water Assessment Tool (SWAT) model using rain gauges and the SPPs in a basin of the Cerrado biome, assessing and comparing the model performances for streamflow simulation.

2. Materials and Methods

2.1. Study Area

The Tocantins-Araguaia river basin (TARB) is the largest basin entirely inserted in the Brazilian territory [6] (Figure 1), accounting for 9% of the country's area [1]. It has a drainage area of the 764,000 km². Furthermore, approximately 64% of the runoff comes from regions where the Cerrado biome is predominant [33]. The TARB is essential for water supply, irrigation, and hydroelectricity generation, being the third-ranked Brazilian basin in installed hydropower, with 13.14 GW comprising 15% of the installed capacity of the country [34]. However, the TARB has the lowest number of rain gauges among the Brazilian basins [35], which undermines the appropriate capture of the spatial distribution of the precipitation and can introduce unknown uncertainties into the estimated spatial precipitation due to the low density of the rain gauge network.

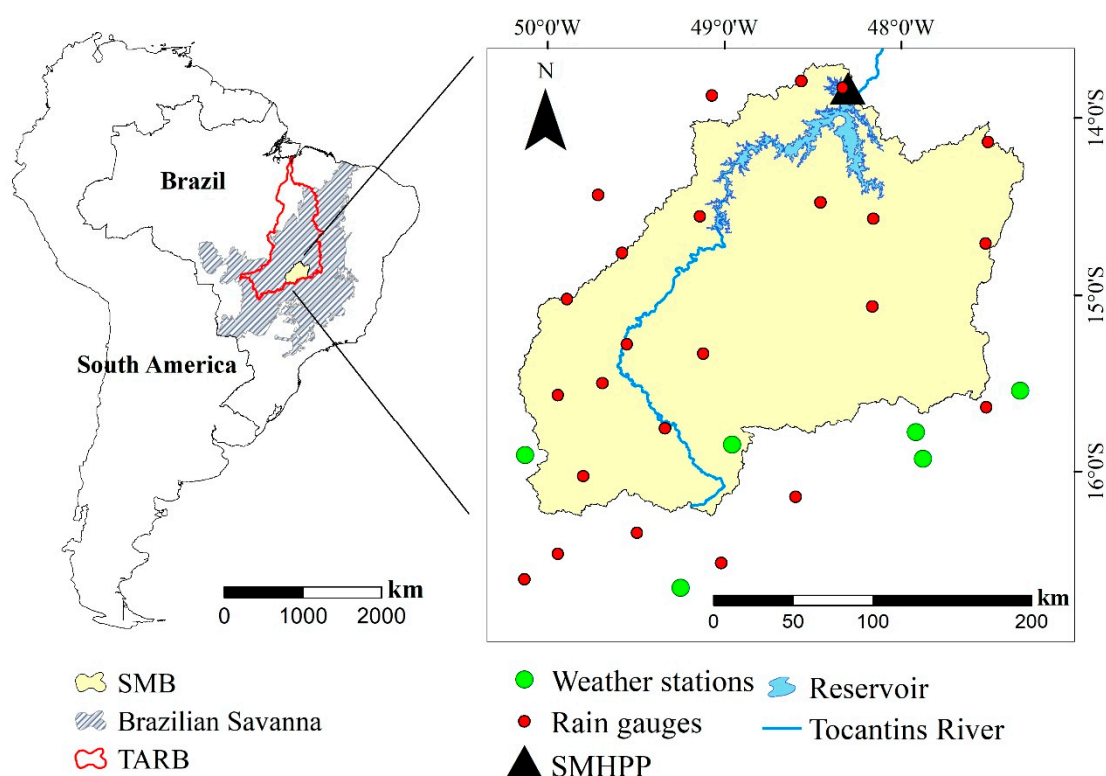


Figure 1. Tocantins-Araguaia River Basin (TARB), Serra da Mesa Basin (SMB), Serra da Mesa Hydropower Plant (SMHPP), weather stations, and rain gauges location.

The study area comprises the upstream drainage area of the Serra da Mesa Hydropower Plant (SMHPP) (Figure 1) in the TARB. The Serra da Mesa Basin (SMB) has a drainage area of 51,238 km² and is responsible for generating 1275 MW, approximately 10% of the total hydroelectricity in the TARB [36]. The SMHPP reservoir has 1784 km² of surface area and is the largest in Brazil in amount of dammed water [37].

According to Koppen's climate classification, the climate of the basin is predominantly Aw (tropical Savanna) with a dry winter [38]. During a long-term climate observed from 1981 to 2010, the average annual precipitation was 1400 mm, the maximum and minimum average annual temperatures were 31 and 18 °C, respectively, and the average annual potential evapotranspiration was 1550 mm. Regarding the topography, the elevation of the SMB ranges between 405 m and 1673 m.

2.2. Precipitation Dataset

2.2.1. Ground-Based Precipitation

Daily precipitation data were obtained from the Brazilian National Institute of Meteorology (INMET) and the Brazilian National Water Agency (ANA—Hidroweb). Precipitation data from 30 rain gauges (Figure 1) were analyzed for consistency evaluation. The criteria adopted for the selection of rain gauges was that they should have less than 10% of missing data in the precipitation time series from June 2000 to December 2018 [6].

2.2.2. Satellite Precipitation Products (SPPs)

The SPP data were obtained from the NASA Goddard Space Flight Center (<https://gpm.nasa.gov>), from which the Tropical Rainfall Measurement Mission (TRMM) and the Global Precipitation Measurement (GPM) products were used (Figure 2). The TRMM is a low-Earth orbit satellite resulting from a joint project between the Japan Aerospace Exploration Agency (JAXA) and the National Aeronautics and Space Administration (NASA) launched in late 1997. The TRMM orbits at an angle of 35° to Ecuador and provides precipitation products between the latitudes of 50° N and 50° S, with temporal resolution varying from three hours to one month and spatial resolutions from 0.25° to 5° [11]. TRMM Multi-satellite Precipitation Analysis (TMPA) is based on the calibration of the products from Infrared (IR), Microwave Passive (MP) wavelength measurements of various satellites, and bias correction of the remote sensing precipitation using rain gauges [11]. In this study, the 7th version of the TMPA (3B42V7) dataset, with a spatial resolution of 0.25° × 0.25° and daily temporal resolution, was used.

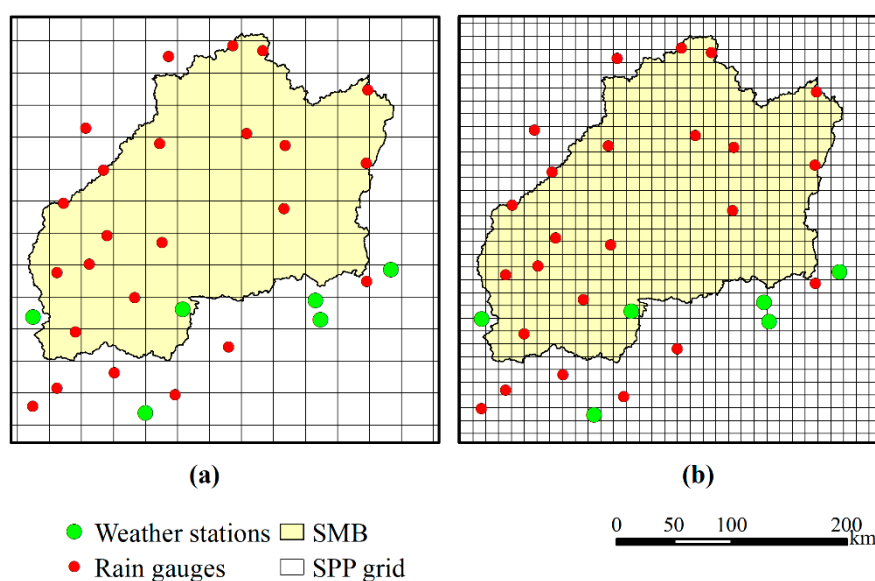


Figure 2. Spatial distribution of weather stations and rain gauges in relation to TRMM Multi-satellite Precipitation Analysis (TMPA) (a) and Integrated Multi-Satellite Retrievals for GPM (IMERG) (b).

The Global Precipitation Measurement (GPM) started with the launch of the GPM Core Observatory in early 2014. GPM is a satellite mission designed to provide a new generation of rainfall observations that are more accurate than the TRMM [10,39]. The GPM Core sensors extend the measurement range attained by the TRMM and provide information globally [39]. Moreover, the Integrated Multi-Satellite Retrievals for GPM (IMERG) provide rainfall and snow information products at 0.1° × 0.1° (spatial) and half-hour (temporal) resolutions to global coverage. IMERG compensates for the low frequency of MP sensors onboard satellites in low-Earth orbits by combining as many satellites as possible with

IR sensors in geocentric orbit [12]. The IMERG dataset used in this study was the IMERG Final Run Version 6 (IMERGF-V6) at a $0.1^\circ \times 0.1^\circ$ (spatial) and daily (temporal) resolution.

2.3. Hydrological Model Description

In this study, the Soil and Water Assessment Tool (SWAT—<http://swat.tamu.edu>) in its 2012 version was used to simulate the streamflow of the SMB. The SWAT is a basin-scale, physically based, semi-distributed, long-term, and continuous-time hydrological model that operates on a daily time step. The SWAT was developed by the US Agricultural Research Service (ARS) to predict the impact on water, sediment production, and agricultural chemicals from land use and management practices [40,41].

The SWAT divides the watershed into multiple subbasins connected by the drainage network based on a Digital Elevation Model (DEM). Each subbasin is further divided into Hydrologic Response Units (HRU) that consist of lumped land comprising unique soil characteristics, land use, management, and topography [40,41].

The water balance, which is the driving force behind the SWAT simulation, is computed for each HRU and accumulated to obtain the total for the subbasins [42]. Equation (1) describes the water balance adopted by the swat model through which the main processes of the hydrological cycle, such as surface and subsurface flows, infiltration, percolation, plant uptake, evapotranspiration, and soil moisture, are obtained.

$$SW_t = SW_0 + \sum_{i=1}^t (R_{\text{day},i} - Q_{\text{surf},i} - E_{a,i} - W_{\text{seep},i} - Q_{\text{gw},i}), \quad (1)$$

where SW_t is the final soil water content (mm H_2O), SW_0 is the initial soil water content on day i (mm); t is the time (days), $R_{\text{day},i}$ is the amount of precipitation on day i (mm), $Q_{\text{surf},i}$ is the amount of surface runoff on day i (mm), $E_{a,i}$ is the amount of evapotranspiration on day i (mm), $W_{\text{seep},i}$ is the amount of water entering the vadose zone from the soil profile on day i (mm), and $Q_{\text{gw},i}$ is the amount of return flow on day i (mm).

The Potential Evapotranspiration (PET) can be computed in the SWAT by the Priestley and Taylor [43], Hargreaves [44], or Penman–Monteith methods [45,46]. The surface runoff is modeled using either the Green–Ampt method [47] or a modification of the Soil Conservation Service (SCS) curve number method (CN-SCS) [48]. The peak flow is obtained by a modified rational method and the flow is routed through the channel using either a variable storage coefficient method or the Muskingum routing method. In this study, the Penman–Monteith, CN-SCS, and variable storage coefficient methods were applied. The SWAT theoretical documentation (Neitsch et al. [49], Arnold et al. [41], and Srinivasan et al. [50]) provide the model equations and detailed description.

2.4. Model Setup

Streamflow simulation in the SWAT requires different types of input data such as the Digital Elevation Model (DEM), soil maps, land use maps, weather, and streamflow data. The river basin delineation, creation of streams, characteristics of the subbasins, and stream network were computed through an Advanced Spaceborne Thermal Emission and Reflection Radiometer (ASTER) DEM with a spatial resolution of 30 m downloaded from the USGS (United States Geological Survey) (Figure 3c).

The soil map (Figure 3a) with a 1:5,000,000 scale used in this study was derived from the Brazilian Agricultural Research Corporation [51]. The soil types in the SMB (Figure 2) are Red Latosol (LV) 31.02%; Litholic Neosol (RL) 18.92%; Red-Yellow Latosol (LVA) 15.13%; Haplic Cambisol (CX) 13.84%; Argiluvic Chernosol (MT) 6.91%; Red-Yellow Podzolic (PVA) 5.85%; Red Podzolic (PV) 5.62%; and Red Nitisol (NV) 2.71%. The land use map (Figure 3b) was provided by the Brazilian Institute of Geography and Statistics [52] at a 1:500,000 scale. The land use in the SMB (Figure 3b) is predominantly Cerrado (Brazilian Savanna), pasture, and agriculture, which represent 67.15%, 22.17%, and 4.56% of the area, respectively, followed by water bodies (3.37%) and forest (2.23%). Urbanization and silviculture account for less than 0.60% of the basin area.

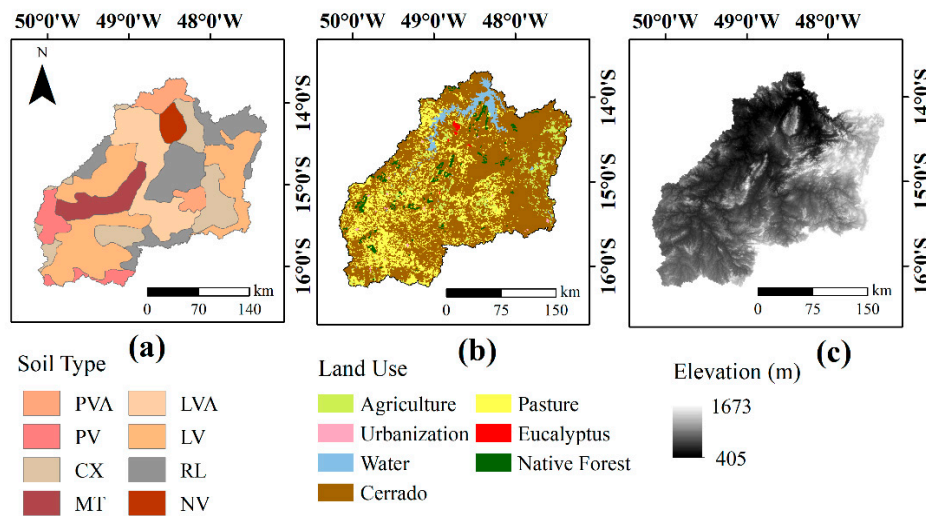


Figure 3. Spatial distribution of (a) soil types (b) and land cover, and (c) Digital Model Elevation (DEM) of the SMB.

Daily weather data from June 2000 to December 2018, such as maximum and minimum temperatures, humidity, wind speed, and solar radiation were taken from six weather stations in the Meteorological Database for Education and Research (BDMEP) of the Brazilian Weather Bureau (INMET) (Figure 1). In the SWAT model, all weather data were categorized into subbasins according to the “nearest-distance” principle [53]. Therefore, a SWAT subbasin will use the weather data from the weather station that is closest to its centroid. The weather data were used in the model simulations for computing the potential evapotranspiration through the Penman–Monteith method. The partition of the precipitation between infiltration and surface runoff was computed using the SCS curve number method and the variable storage coefficient method was used for routing in the channel.

The grids containing the SPP data (TMPA and IMERG) were delimited using the boundaries of the basin and transformed into points representing the centroid of each pixel. The historical series of daily precipitation obtained at each point of the SPPs were used as input in the SWAT. For the hydrological simulation, 460 and 79 points were used within the basin area from IMERG and TMPA, respectively. Similar to the weather data, both SPP and rain gauge data were categorized into subbasins according to the “nearest-distance” principle.

Due to the presence of the reservoir in the basin, the naturalized streamflow data from the SMHPP were obtained from the National Electric System Operator (ONS) and used for comparison between the SWAT model simulation results. Naturalized streamflows are those that occur if there is no reservoir in a basin [54], and they are derived from an integrated system that incorporates 96 stochastic models for forecasting the streamflows in each hydropower plant [55]. Naturalized streamflows have been used in several studies of hydrological modeling in Brazil, such as those by Cassalho et al. [13], Nóbrega et al. [56], and Oliveira et al. [55].

2.5. Calibration and Validation of the SWAT Model

The calibration, validation, and uncertainty analysis were carried out automatically using the program SWAT Calibration and Uncertainty Procedures (SWAT-CUP) [57]. Among different calibration algorithms in SWAT-CUP, the Sequential Uncertainty Fitting algorithm (SUFI-2) was used in this study with Nash–Sutcliffe efficiency (NSE) as an objective function.

The SUFI-2 algorithm [53,58] expresses all uncertainties, such as uncertainty in the conceptual model, drive variables, and measured data, within the parameter ranges, and attempts to capture most of the measured data within the 95% prediction uncertainty (95PPU) of the model in an iterative process [59]. The 95% prediction uncertainty is calculated at 2.5% and 97.5% levels of the cumulative distribution of an output variable obtained by sampling in a Latin hypercube. Both p-factor (percentage

of observation within the 95PPU band) and r-factor (which corresponds to the average thickness of the 95PPU band divided by the standard deviation of the measured data) were used to evaluate the uncertainty of the simulation. Although there are no exact numbers for what these two factors should be, Abbaspour et al. [59] suggested a p-factor greater than 0.7 (>70%) and an r-factor around 1 for streamflow simulation.

The streamflow simulation was performed for the period from June 2000 to December 2018. In large basins, the water resources management and planning are carried out monthly, and the observed hydrological data, which are then more readily available, are used for calibrating and validating hydrological models [55]. The first two years were used as a warm-up period to reduce the uncertainties regarding the initial conditions of the surface domain [60]. The period from January 2002 to December 2010 was used for calibration. The initial ranges of the parameters used in calibration were selected based on previous studies conducted in the Cerrado biome, such as Oliveira et al. [27] and Rodrigues et al. [61]. Subsequently, the parameters were adjusted for the study area through two iterations with 500 simulations each through the SUFI-2 algorithm implemented in SWAT-CUP. The validation consisted of running the model from January 2011 to December 2018 using the parameters adjusted in the calibration period.

2.6. Meteorological and Hydrological Evaluation

The performance of the SPPs was divided into precipitation assessment (comparison with rain gauges) and hydrological assessment (comparing the validation of SWAT streamflow simulations and observed streamflow). As the pixel-to-pixel approach requires a high density of rain gauges [62], uncertainties may arise from the interpolation of data due to the low density of rain gauges [63]. Furthermore, the spatial resolutions of TMPA and IMERG are different, which can affect the comparison. For this reason, the point-to-pixel approach was used to compare the precipitation rain gauges against SPPs in this study [62–65]. In this approach, the rain gauges closest to the centroid of the SPP grid pixel were compared with SPPs on a daily and monthly basis. The performance of the SPPs was assessed through statistical metrics (Table 1), including the root mean square error (RMSE), percentage bias (Pbias), correlation coefficient (r), and Kling–Gupta efficiency (KGE) [66].

Table 1. Statistical metrics for hydrological and meteorological assessment.

Statistical Metrics	Equation	Perfect Value	Unit
Root mean square error	$RMSE = \sqrt{\frac{\sum_{i=1}^n (P_i - O_i)^2}{n}}$	0	mm
Correlation coefficient	$r = \frac{\sum_{i=1}^n (O_i - \bar{O})(P_i - \bar{P})}{\sqrt{\sum_{i=1}^n (O_i - \bar{O})^2} \sqrt{\sum_{i=1}^n (P_i - \bar{P})^2}}$	1	NA
Percentage bias	$PBIAS = \frac{\sum_{i=1}^n (O_i - P_i)}{\sum_{i=1}^n O_i} \times 100$	0	%
Kling–Gupta efficiency	$KGE = 1 - \sqrt{(r - 1)^2 + (\beta - 1)^2 + (\gamma - 1)^2}$ $\beta = \frac{\bar{P}}{\bar{O}} \quad \gamma = \frac{\sigma_P / \bar{P}}{\sigma_O / \bar{O}}$	1	NA
Nash–Sutcliffe Efficiency	$NSE = 1 - \left[\frac{\sum_{i=1}^n (O_i - P_i)^2}{\sum_{i=1}^n (O_i - \bar{O})^2} \right]$	1	NA

\bar{P} and \bar{O} are the average of the estimated and observed variable, respectively; P_i and O_i are the i^{th} estimated and observed variable, respectively; n is the number of observations; and σ_P and σ_O are the standard deviation of the estimated and observed variable, respectively.

The hydrological assessment of the SPPs was carried out by comparing the SWAT streamflow simulation using the different precipitation inputs (rain gauges, TMPA, and IMERG). In addition to the uncertainty analysis performed using the p-factor and r-factor described in Section 2.5, the Pbias, NSE, and KGE (Table 1) were adopted to evaluate the model’s performance regarding the calibration and validation periods. The evaluation criteria considered in this study was proposed by Moriasi et al. [67]:

“very good” ($NSE > 0.75$; $PBIAS < \pm 10$), “good” ($0.65 < NSE < 0.75$; $\pm 10 < PBIAS < \pm 15$), “satisfactory” ($0.50 < NSE < 0.65$; $\pm 15 < PBIAS < \pm 25$), and “unsatisfactory” ($NSE < 0.50$; $PBIAS > \pm 25$). In addition, the KGE closest to 1 indicates the best fit of the model [66].

3. Results

3.1. Validation of SPP against Rain Gauges

Figure 4 shows the box plots of the statistical metrics as well as the points representing the result of the comparison between SPPs against rain gauge over the SMB on a daily and monthly basis. Overall, IMERG and TMPA presented similar results at both time scales. The average Pbias indicates that IMERG presented more overestimation than TMPA on a daily (Pbias of -3.13% and -0.34% , respectively) and monthly time scale (Pbias of -3.56% and -0.75% , respectively). The highest overestimations for IMERG and TMPA were 40.20% and 37.80% , respectively, at both time scales. On the other hand, the underestimation reached 28.7% and 33.3% for IMERG and TMPA, respectively.

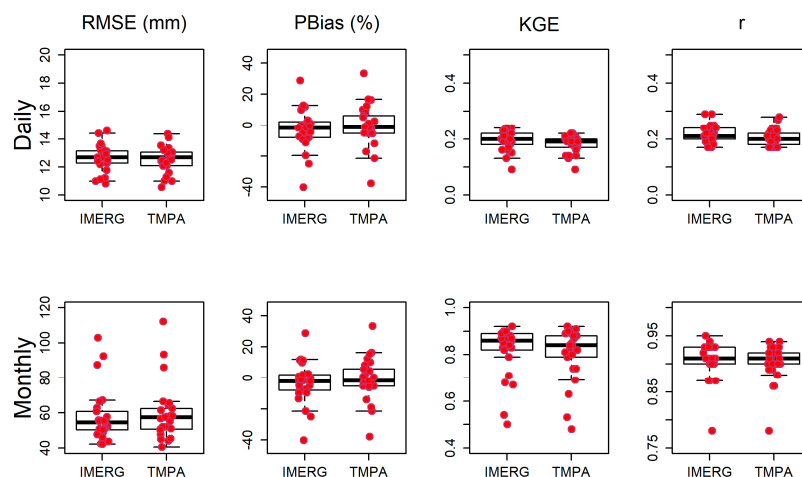


Figure 4. Boxplot of the statistical metrics on a daily and monthly time scale for all rain gauges over the SMB.

The magnitude of error between SPPs and rain gauges presented by the RMSE showed similar values, mainly daily time scale, in which the average RMSEs for IMERG and TMPA were 12.65 and 12.54 mm, respectively. However, a better performance for the average RMSE was obtained on a monthly time scale by IMERG (58.09 mm) in comparison to TMPA (59.61 mm). In addition, the coefficient of correlation (r) highlighted the greater performance of IMERG. Both TMPA and IMERG showed a lower correlation with gauges on a daily time scale. Despite varying at similar magnitudes, the monthly average r value of IMERG was greater than TMPA, being 0.91 and 0.90, respectively. As a result, the precipitation derived from IMERG presented a slightly better agreement with rain gauges than TMPA. For KGE, the results ranged from 0.09 to 0.24 for IMERG, and from 0.09 to 0.22 for TMPA, when the comparison was performed on a daily scale. Similar to the r values, average KGE values increased on a monthly scale, ranging from 0.50 to 0.92 for IMERG and from 0.48 to 0.92 for TMPA. The average KGE values of IMERG were slightly better than TMPA.

3.2. Monthly Streamflow Simulation Using SPP and Rain Gauges

Table 2 presents the parameters that were used in the SWAT model with their respective initial ranges, which were selected from the literature review of hydrological modeling studies in the Brazilian Cerrado biome [27,61], and the range of the parameters obtained by SUFI2. It is interesting to highlight that the simulations driven by IMERG and rain gauges resulted in similar parameter values. A detailed description of the parameters used in this study can be obtained in Neitsch et al. [49].

Table 2. Statistical metrics for hydrological and meteorological assessment.

Parameter	Initial Range	Rain Gauges		TMPA		IMERG	
		Final Range	Best Fit	Final Range	Best Fit	Final Range	Best Fit
esco.hru ¹	0.5–0.95	0.5–0.77	0.548	0.5–0.91	0.617	0.5–0.77	0.548
cn2.mgt ²	(–0.2)–0.2	(–0.2)–0.011	–0.06	(–0.2)–0.025	–0.13	(–0.2)–0.0114	–0.06
alpha_bf.gw ¹	0–0.01	0.0038–0.01	0.009	0.0047–0.01	0.0095	0.0038–0.01	0.009
gw_delay.gw ³	(–30)–60	(–8.454)–37.194	–2.02	(–26.814)–31.074	–24.44	(–8.454)–37.194	–2.02
gwqmn.gw ³	(–1000)–1000	(–83.202)–1000	916.6	(–377.201)–869.201	–301.2	(–83.202)–1000	916.6
canmx.hru ¹	0–50	16.2–48.83	45.411	18.8–50	33.104	16.2–48.83	45.411
ch_k2.rte ¹	(–0.01)–10	3.50–10	7.915	3.82–10	4.183	3.50–10	7.913
ch_n2.rte ¹	(–0.01)–0.3	0.086–0.278	0.195	0.0763–0.249	0.208	0.086–0.279	0.195
epco.bsn ¹	0.01–1	0.388–1	0.976	0.01–0.517	0.450	0.388–1	0.976
gw_revap.gw ¹	0.02–0.2	0.088–0.2	0.1708	0.0431–0.1477	0.1315	0.088–0.2	0.1708
revapmn.gw ³	0–500	198.699–500	320.1	0–295.299	240.1	198.700–500	320.1
sol_awc.sol ²	(–0.1)–0.1	(–0.008)–0.1	0.074	(–0.1)–0.00012	–0.001	(–0.008)–0.1	0.074
sol_k.sol ²	(–0.1)–0.1	(–0.0145)–0.1	0.045	(–0.1)–0.0015	–0.090	(–0.015)–0.1	0.045
surlag.bsn ¹	0.01–24	0.01–14.19	5.181	0.01–14.80	11.385	0.01–14.19	5.181

^{1,2,3} correspond to the operations replace, relative, and addition, respectively.

The results of the statistical metrics used to evaluate SWAT performance are shown in Table 3. The criteria presented by Moriasi et al. [67] were used to interpret the SWAT's performance. Regarding the NSE values, the performance of the model forced with rain gauges (ground precipitation), IMERG, and TMPA was considered “very good” for both calibration and validation.

Table 3. Statistical metrics of SWAT streamflow simulation for both calibration and validation periods.

Index	Rain Gauges		TMPA		IMERG	
	Calibration	Validation	Calibration	Validation	Calibration	Validation
NSE	0.86	0.84	0.85	0.82	0.82	0.83
Pbias	–13.2	–23.6	–11.4	–12.7	–2.6	–12.3
KGE	0.82	0.75	0.87	0.85	0.79	0.80
p-factor	0.75	0.69	0.88	0.78	0.73	0.76
r-factor	0.97	1.01	0.84	0.80	0.94	0.95

In terms of Pbias values, simulations driven by the SPPs performed better than the simulations driven by rain gauges. Both calibration and validation periods driven by SPPs presented performances classified as “good”, except for the validation using IMERG that was classified as “very good”. On the other hand, simulations based on rain gauges presented inferior performances. Although the simulation driven by rain gauges was classified as “good” in the calibration, the performance of the model in the validation period was lower and classified only as “satisfactory” (Pbias of –23.6%). As a result, the SWAT showed a more significant overestimation of the observed data when driven with rain gauges.

KGE results closest to 1 indicate the perfect adjustment between observed and simulated data. The simulations with TMPA showed better performance both in the calibration and validation periods (Table 3). The simulation driven by IMERG presented similar KGE values for calibration and validation, whereas simulations forced by rain gauges obtained higher KGEs in calibration than in the validation period (0.82 and 0.75, respectively).

Through the p-factor and r-factor (Table 3), it is possible to observe that all simulations presented low uncertainties according to the criteria suggested by Abbaspour et al. [59]. The results showed that the simulation using TMPA presented more reliable results than other precipitation inputs, whereas the validation of the simulation using rain gauges presented the highest uncertainty among the inputs, in which the p-factor was slightly lower than 0.7.

Although IMERG has higher statistical coefficients, the uncertainty analysis and scatters plots (Figure 5) indicate a better performance of TMPA for water resource management concerning recession

streamflow. Figure 5 shows that the simulation based on IMERG underestimates peak streamflow, indicating that the use of this product in flood mitigation studies could lead to errors.

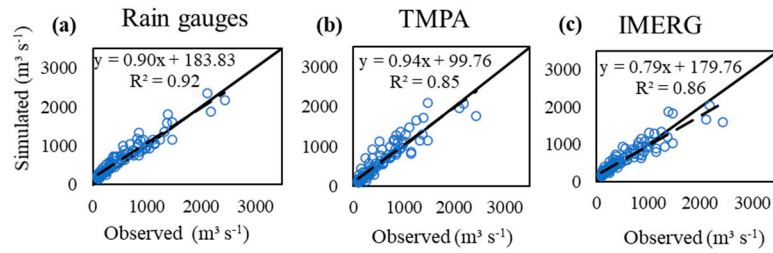


Figure 5. Scatter plots of the observed and simulated streamflows using different precipitation data sources.

The results depicted in Figure 6 show that the recession periods in the simulations driven by TMPA were better represented than both IMERG and rain gauges. This fact becomes clearer in the monthly streamflow duration curve (Figure 7), in which the streamflows with exceeding frequencies (duration) above 70% using TMPA were closer to the observed streamflow than other rainfall sources.

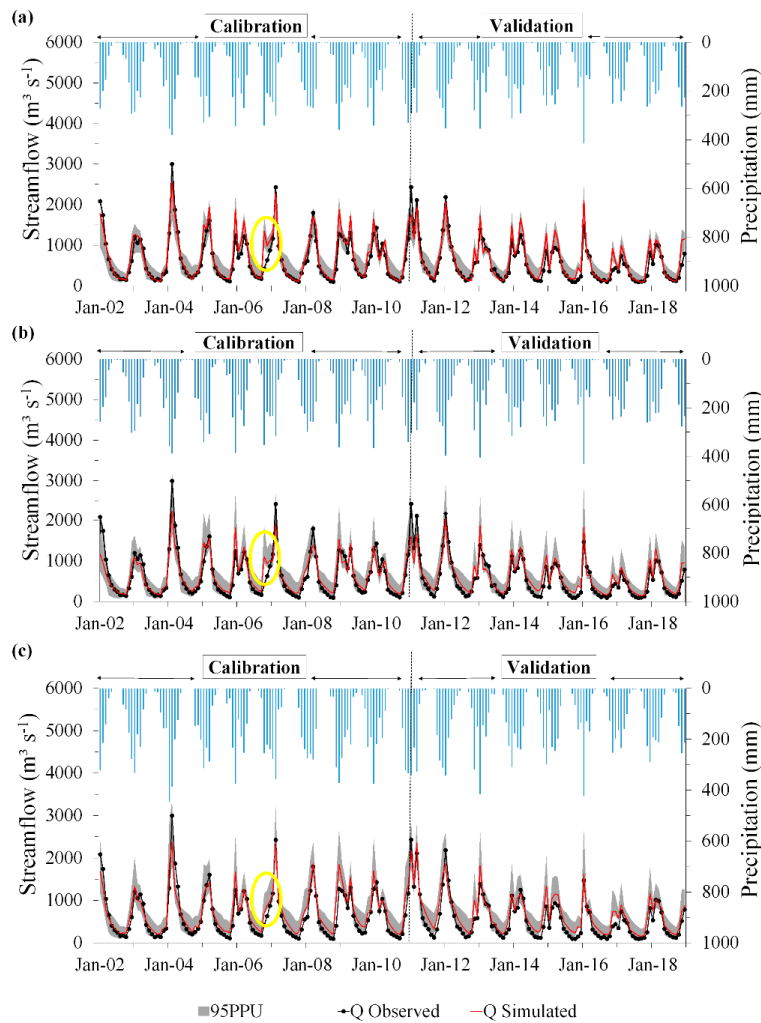


Figure 6. Observed 95% prediction uncertainty (95PPU) and simulated monthly streamflow driven by (a) TMPA, (b) IMERG, and (c) rain gauges. The yellow circle represents an anomaly in the simulated streamflow driven by SPPs.

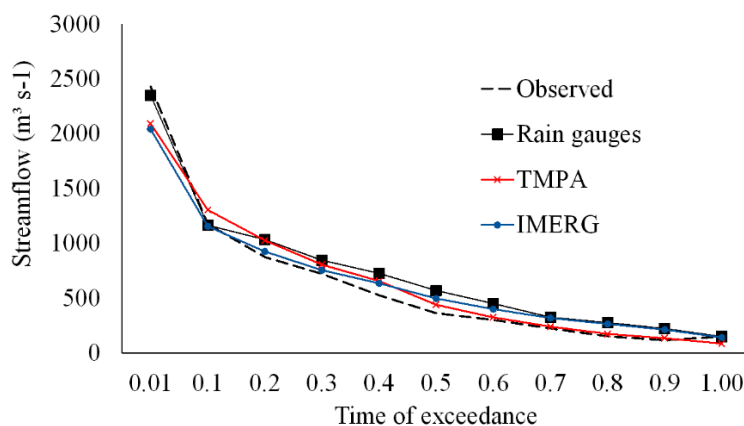


Figure 7. Monthly permanent streamflow curves using different rainfall sources and observed values.

4. Discussion

4.1. Meteorological Evaluation

The critical aspect of the SPP evaluation was the difference in spatial resolution between SPPs and rain gauges. Although Tan et al. [62] found no difference between the two approaches when comparing point-to-pixel and pixel-to-pixel in a basin located in Malaysia, the point-to-pixel approach may have been compromised due to the spatial difference between precipitation data sources and the low density of the rain gauges in the SMB, as shown in Figure 2. Furthermore, since satellite measurements represent the average value within a pixel observed in the atmosphere, whereas rain gauges generally collect point precipitation observed on the ground [62], the limitations of point-to-pixel can increase these differences [68].

RMSE, PBIAS, KGE, and r statistic metrics were used to assess the ability of TMPA and IMERG to represent the rainfall. Overall, both IMERG and TMPA were able to estimate rainfall in the Cerrado biome region on a monthly time scale more accurately than on a daily scale (Figure 4). Since the final versions of both SPPs were used in this study, the monthly bias corrections applied to these products before being made available may explain the best performance when used on a monthly scale. For statistical metrics referring to bias and magnitude of error, the behavior was similar to the daily data.

Gadelha et al. [7] evaluated IMERG over Brazil on a monthly basis and obtained r values higher than 0.80 in 90% of the cells on a monthly time scale, whereas a large number of cells presented r values ranging from 0.1 to 0.6 on a daily scale in central-western Brazil, where the SMB is located. The results confirmed that the use of longer time averages such as a monthly scale are more representative of the comparison between SPPs and rain gauges in Brazil. Melo et al. [15] also obtained better statistical metrics for TMPA over Brazil when evaluating on a monthly scale. Better results are expected on a monthly time scale since both IMERG and TMPA are corrected with ground precipitation data to remove monthly bias [11].

Despite improvements presented from the removal of bias, the results of PBIAS for both SPPs showed an overestimation of the observed precipitation in both time scales. Similar results were obtained in other regions of the world. Su et al. [69], in a study performed with IMERG, found a slightly higher overestimation of the precipitation over Mainland China. Results obtained by Rozante et al. [70] indicate IMERG and TMPA products overestimate precipitation over Brazil.

Although TMPA presented an average PBIAS value closer to zero, and showed better performance than IMERG, TMPA also showed an overestimation of precipitation over the SMB. Other studies also point to the overestimation of the precipitation estimated from TMPA. Falck et al. [1] observed overestimations of precipitation obtained from TMPA when compared to rain gauges over the Tocantins-Araguaia river basin. A similar result was obtained by Melo et al. [15] in an assessment of

the general quality of TMPA 3B42 (versions 6 and 7, available at <https://disc.gsfc.nasa.gov/>) estimates over Brazil. The authors found a high level of uncertainty in the estimates of the precipitation in central-western Brazil. Despite the improvements in the 6th version compared to the 5th, it should be noted that TMPA still presented difficulties in estimating the precipitation of the Cerrado biome region.

RMSE, r , and KGE indicate that IMERG performed slightly better than TMPA in the SMB. This result can be attributed to the increasing number of passive microwave samples for measurements compared to TMPA [39]. Microwave passives samples are more accurate than infrared, and they are visible because of their sensitivity to the concentrations of ice particles or droplets associated with precipitation [71]. In addition, IMERG is more sensitive in light rainfall than TMPA, since the DPR in GPM has a sensitivity of 0.2 mm h^{-1} in the Ka-band, whereas the Precipitation Radar (PR) in the TRMM is 0.5 mm h^{-1} . Furthermore, according to Prakash et al. [4], the DPR can detect and estimate extreme precipitation more precisely than PR. The best performance demonstrated by IMERG rather than TMPA was also observed in other studies [8,63,69]. In Brazil, Rozante et al. [70] also showed that IMERG presented results that were superior to TMPA.

The r and KGE metrics showed similar results for IMERG and TMPA. However, a greater correlation was obtained between IMERG and the observed precipitation. Thus, since the TMPA data were interrupted in 2019, IMERG has presented as a potential substitute for satellite precipitation monitoring in the Cerrado biome.

4.2. SWAT Performance Evaluation

Based on the statistical metrics NSE and Pbias, IMERG performed better among the precipitation data sources. The results obtained in this study were more accurate than those found by Monteiro et al. [6] in the Tocantins river basin, in which the SWAT was driven using remote sensing products from climatic reanalysis, Climate Forecast System Reanalysis (CFSR), and ERA-Interim. Both TMPA and IMERG performed better than the reanalysis products for the validation period.

The NSE values (Table 3) indicate that both IMERG and TMPA were able to simulate streamflow in the SMB. However, greater NSE values were obtained from IMERG. As in the Cerrado biome, studies highlighted the hydrological relevance of IMERG as well as of TMPA. Le et al. [8] simulated the monthly streamflow in six representative river basins in Vietnam, covering six sub-climate zones, using the SWAT and the SPPs TMPA, IMERG, Climate Hazards Group Infrared Precipitation with Station (CHIRPS), and Precipitation Estimation from Remotely Sensed Information using Artificial Neural Networks (PERSIANN). The median NSEs obtained for all basins were 0.77 and 0.74, using IMERG and TMPA, respectively. Jiang et al. [72] performed the hydrological simulations using IMERG in comparison with TMPA over the mid-latitude humid Mishui basin in southern China. They concluded that, overall, IMERG demonstrated the best performance (NSE of 0.78), presenting a potential alternative for water resource planning and management.

Hydrological simulation with the three products overestimated the streamflow presenting negative Pbias values. The inferior performances of the simulations were observed when rain gauges were used. IMERG performed better during the calibration period, whereas the results were close to those obtained with TMPA during the validation. TMPA was able to better simulate the minimum streamflows (Figures 6 and 7) and peak streamflows (Figure 5), and thus was more suitable for the calculation of minimum streamflows (which are very important for water use in Brazil) as well as flood studies. Furthermore, since KGE offers interesting results in model performance evaluation because it uses correlation, variability, and bias [73], its values showed the best SWAT performance when coupled with TMPA.

Overall, SWAT streamflow simulations using SPPs and rain gauges presented satisfactory performances regarding uncertainty analysis. Zhu et al. [74] highlighted that uncertainty analysis is necessary to evaluate the hydrological applications of SPP datasets, since the influence of parameter uncertainty on model simulation may be greater than the effects of input data accuracy. Despite presenting adequate r-factor values (Table 3), the simulation driven by rain gauges presented

higher uncertainty when compared to the SPPs, presenting a p-factor slightly lower than 0.7 for the validation period. According to Cassalho et al. [13], the local characteristic of rain gauges often limits their ability to represent the spatial structure of precipitation events. Therefore, the low density of rain gauges may be the cause of the greater uncertainties in the simulations [75].

The p-factor values for the simulations driven by TMPA were slightly larger than other precipitation sources (Table 3). It is possible to assume from the p-factor values that the 95PPU band of the simulation using TMPA (Figure 6) was capable of capturing 88% and 78% of the observed streamflows for calibration and validation, respectively. Furthermore, the r-factor values both for calibration and validation (0.84 and 0.80, respectively) were lower than those obtained with other precipitation data. Consequently, a narrower 95PPU band was generated, and less uncertainty in the fitted parameters was obtained from TMPA (Figure 6).

A higher p-factor and consequently a larger width of 95PPU could be achieved if the r-factor were high. However, greater uncertainties in outputs may arise. Hence, a balance should be reached between the two factors [59]. In this sense, a study conducted by Silva et al. [76] in three basins in the Brazilian Cerrado biome obtained larger uncertainties in streamflow simulations using the SWAT driven by rain gauges. In the validation period, the r-factor values were 1.74, 2.35, and 3.44, whereas p-factor values were 0.87, 0.86, and 0.81, respectively [76]. This result emphasizes the reliability of SPPs for hydrological simulation in the SMB when compared with rain gauges.

The 95PPU band from the simulations driven by IMERG was capable of capturing 73% and 76% of the observed values for calibration and validation, respectively (Table 3), and presented greater uncertainties than TMPA. Such uncertainties were greater in the simulation of the recession phase of the hydrographs (dry periods), both in calibration and validation periods (Figure 6). It is possible to observe that the 95PPU band did not include the recessions that occurred in the years 2015 and 2016 the observed data. In these years, Junqueira et al. [77] observed one of the most severe droughts in the basin for the 1987–2017 period, which may have affected SWAT performance.

An anomaly in the simulations driven by SPPs was observed in October 2006 (Figure 6). Since an anomaly did not occur in the simulation driven by rain gauges, and the only difference between the model setups was the precipitation data inputs, this occurrence may have been due to false alarms (i.e., when there is no precipitation recorded in rain gauges, but the satellite product records a value). As noticed by Prakash et al. [4] in southeast peninsular India, and Gadelha et al. [7] in Brazil, false alarms are probably caused by low numbers of rainy days in certain periods of the year, a situation that is normal from May to September (dry season) in the SMB.

IMERG offers a great potential for monitoring rainfall and hydrological studies in the Brazilian Cerrado biome, and is an alternative to TMPA. The high spatial resolution provided by SPPs is a significant improvement for hydrological simulations in the region with a deficient ground base rainfall monitoring. Furthermore, an improvement in IMERG data for hydrological studies can be achieved with the application of rainfall data merging methods. Neirini et al. [78] compared two non-parametric rainfall data merging methods for optimizing the hydrometeorological performance of SPPs over a tropical watershed and obtained improvements in hydrological performance over the original SPP. Thus, it is expected that the rainfall data merging methods will increase the performance of IMERG in hydrological applications and the reliable usage in the management of water resources in the Cerrado biome.

5. Conclusions

The low density of rain gauges used for validating SPPs may have been one of the reasons for some errors obtained in the study area. A greater number of gauges would provide information for a more adequate assessment of the ability of SPPs to capture the spatial variability of precipitation in the study area. Both SPPs showed similar performances in monitoring rainfall. However, the statistical metrics highlighted a slightly better performance for IMERG on daily and monthly time scales. The bias

removal performed in both the final TMPA and IMERG versions was the main reason for the strong agreement between SPPs and rain gauges explained by KGE and r .

Overall, SPPs and rain gauges were able to simulate the hydrological regime in the SMB. The simulations driven by rain gauges showed higher overestimations than SPPs. The better performance of SPP products is associated with the finer spatial resolution in precipitation measurements, since the rainfall monitoring in the ground is sparse in the SMB. TMPA showed less uncertainty in the hydrological simulations (p -factor and r -factor) and more adequately captured hydrological behavior than IMERG. IMERG showed less ability than TMPA in simulating peak streamflows, which may compromise its application for some purposes such as flood forecasting. The rainfall data merging methods may assist in overcoming this limitation and could improve SPP performance.

IMERG demonstrated a strong potential for replacing TMPA in the estimation of precipitation over the SMB since TMPA was discontinued in 2019. In addition, SPPs present a potential application for hydrological modeling and water resource management in the Brazilian Cerrado biome.

Author Contributions: Conceptualization, J.d.S.A. and M.R.V.; Data curation, J.d.S.A.; Methodology, J.d.S.A. and M.R.V.; Supervision, J.d.S.A., M.R.V., and C.R.d.M.; Writing—original draft, J.d.S.A., M.R.V., R.J., V.A.d.O., and C.R.d.M.; Writing—review & editing, J.d.S.A., M.R.V., R.J., V.A.d.O., and C.R.d.M. All authors have read and agreed to the published version of the manuscript.

Funding: We would like to thank the Coordenação de Aperfeiçoamento de Pessoal de Nível Superior—CAPES for the scholarships granted to the authors J.d.S.A. [grant number 88882.446854/2019-01], R.J. [grant number 88882.446869/2019-01], and V.A.d.O. [grant number 88882.306661/2018-01].

Acknowledgments: We greatly acknowledge the Brazilian National Water Agency (ANA), the Brazilian National Institute of Meteorology (INMET), and the National Aeronautics and Space Administration (NASA) for providing the input data to develop this study. We also acknowledge CAPES for granting scholarships to the first, third, and fourth authors, and CNPq for granting fellowship of research productivity (PQ) to the second and fifth authors.

Conflicts of Interest: The authors declare no conflict of interest.

References

1. Falck, A.S.; Maggioni, V.; Tomasella, J.; Vila, D.A.; Diniz, F.L.R. Propagation of satellite precipitation uncertainties through a distributed hydrologic model: A case study in the Tocantins–Araguaia basin in Brazil. *J. Hydrol.* **2015**, *527*, 943–957. [[CrossRef](#)]
2. Hobouchian, M.P.; Salio, P.; García Skabar, Y.; Vila, D.; Garreaud, R. Assessment of satellite precipitation estimates over the slopes of the subtropical Andes. *Atmos. Res.* **2017**, *190*, 43–54. [[CrossRef](#)]
3. Tapiador, F.J.; Turk, F.J.; Petersen, W.; Hou, A.Y.; García-Ortega, E.; Machado, L.A.T.; Angelis, C.F.; Salio, P.; Kidd, C.; Huffman, G.J.; et al. Global precipitation measurement: Methods, datasets and applications. *Atmos. Res.* **2012**, *104–105*, 70–97. [[CrossRef](#)]
4. Prakash, S.; Mitra, A.K.; AghaKouchak, A.; Liu, Z.; Norouzi, H.; Pai, D.S. A preliminary assessment of GPM-based multi-satellite precipitation estimates over a monsoon dominated region. *J. Hydrol.* **2018**, *556*, 865–876. [[CrossRef](#)]
5. Salio, P.; Hobouchian, M.P.; García Skabar, Y.; Vila, D. Evaluation of high-resolution satellite precipitation estimates over southern South America using a dense rain gauge network. *Atmos. Res.* **2015**, *163*, 146–161. [[CrossRef](#)]
6. Monteiro, J.A.F.; Strauch, M.; Srinivasan, R.; Abbaspour, K.C.; Gücker, B. Accuracy of grid precipitation data for Brazil: Application in river discharge modelling of the Tocantins catchment. *Hydrol. Process.* **2016**, *30*, 1419–1430. [[CrossRef](#)]
7. Gadelha, A.N.; Coelho, V.H.R.; Xavier, A.C.; Barbosa, L.R.; Melo, D.C.D.; Xuan, Y.; Huffman, G.J.; Petersen, W.A.; Almeida, C.D.N. Grid box-level evaluation of IMERG over Brazil at various space and time scales. *Atmos. Res.* **2019**, *218*, 231–244. [[CrossRef](#)]
8. Le, M.H.; Lakshmi, V.; Bolten, J.; Bui, D. Du Adequacy of Satellite-derived Precipitation Estimate for Hydrological Modeling in Vietnam Basins. *J. Hydrol.* **2020**, *586*, 124820. [[CrossRef](#)]

9. De Paiva, R.C.D.; Buarque, D.C.; Collischonn, W.; Bonnet, M.-P.; Frappart, F.; Calmant, S.; Bulhões Mendes, C.A. Large-scale hydrologic and hydrodynamic modeling of the Amazon River basin. *Water Resour. Res.* **2013**, *49*, 1226–1243. [[CrossRef](#)]
10. Wang, Z.; Zhong, R.; Lai, C.; Chen, J. Evaluation of the GPM IMERG satellite-based precipitation products and the hydrological utility. *Atmos. Res.* **2017**, *196*, 151–163. [[CrossRef](#)]
11. Huffman, G.J.; Bolvin, D.T.; Nelkin, E.J.; Wolff, D.B.; Adler, R.F.; Gu, G.; Hong, Y.; Bowman, K.P.; Stocker, E.F. The TRMM Multisatellite Precipitation Analysis (TMPA): Quasi-Global, Multiyear, Combined-Sensor Precipitation Estimates at Fine Scales. *J. Hydrometeorol.* **2007**, *8*, 38–55. [[CrossRef](#)]
12. Huffman, G.J.; Bolvin, D.T.; Nelkin, E.J.; Tan, J. Integrated Multi-satellite Retrievals for GPM (IMERG) Technical Documentation. *J. ISMAC* **2019**, *1*. [[CrossRef](#)]
13. Cassalho, F.; Daleles Rennó, C.; Bosco Coura dos Reis, J.; Cláudio da Silva, B. Hydrologic Validation of MERGE Precipitation Products over Anthropogenic Watersheds. *Water* **2020**, *12*, 1268. [[CrossRef](#)]
14. Collischonn, B.; Collischonn, W.; Tucci, C.E.M. Daily hydrological modeling in the Amazon basin using TRMM rainfall estimates. *J. Hydrol.* **2008**, *360*, 207–216. [[CrossRef](#)]
15. de Melo, D.C.D.; Xavier, A.C.; Bianchi, T.; Oliveira, P.T.S.; Scanlon, B.R.; Lucas, M.C.; Wendland, E. Performance evaluation of rainfall estimates by TRMM Multi-satellite Precipitation Analysis 3B42V6 and V7 over Brazil. *J. Geophys. Res. Atmos.* **2015**, *120*, 9426–9436. [[CrossRef](#)]
16. Coelho, V.H.R.; Montenegro, S.; Almeida, C.N.; Silva, B.B.; Oliveira, L.M.; Gusmão, A.C.V.; Freitas, E.S.; Montenegro, A.A.A. Alluvial groundwater recharge estimation in semi-arid environment using remotely sensed data. *J. Hydrol.* **2017**, *548*, 1–15. [[CrossRef](#)]
17. Worqlul, A.W.; Yen, H.; Collick, A.S.; Tilahun, S.A.; Langan, S.; Steenhuis, T.S. Evaluation of CFSR, TMPA 3B42 and ground-based rainfall data as input for hydrological models, in data-scarce regions: The upper Blue Nile Basin, Ethiopia. *Catena* **2017**, *152*, 242–251. [[CrossRef](#)]
18. Tang, G.; Zeng, Z.; Long, D.; Guo, X.; Yong, B.; Zhang, W.; Hong, Y. Statistical and Hydrological Comparisons between TRMM and GPM Level-3 Products over a Midlatitude Basin: Is Day-1 IMERG a Good Successor for TMPA 3B42V7? *J. Hydrometeorol.* **2016**, *17*, 121–137. [[CrossRef](#)]
19. Zubieta, R.; Getirana, A.; Espinoza, J.C.; Lavado-Casimiro, W.; Aragon, L. Hydrological modeling of the Peruvian-Ecuadorian Amazon Basin using GPM-IMERG satellite-based precipitation dataset. *Hydrol. Earth Syst. Sci.* **2017**, *21*, 3543–3555. [[CrossRef](#)]
20. Amjad, M.; Yilmaz, M.T.; Yucel, I.; Yilmaz, K.K. Performance evaluation of satellite- and model-based precipitation products over varying climate and complex topography. *J. Hydrol.* **2020**, *584*, 124707. [[CrossRef](#)]
21. Dinku, T.; Chidzambwa, S.; Ceccato, P.; Connor, S.J.; Ropelewski, C.F. Validation of high-resolution satellite rainfall products over complex terrain. *Int. J. Remote Sens.* **2008**, *29*, 4097–4110. [[CrossRef](#)]
22. Hu, Q.; Yang, D.; Wang, Y.; Yang, H. Accuracy and spatio-temporal variation of high resolution satellite rainfall estimate over the Ganjiang River Basin. *Sci. China Technol. Sci.* **2013**, *56*, 853–865. [[CrossRef](#)]
23. Jiang, S.H.; Ren, L.L.; Yong, B.; Yang, X.L.; Shi, L. Evaluation of high-resolution satellite precipitation products with surface rain gauge observations from Laohahe Basin in northern China. *Water Sci. Eng.* **2010**, *3*, 405–417. [[CrossRef](#)]
24. Eini, M.R.; Javadi, S.; Delavar, M.; Monteiro, J.A.F.; Darand, M. High accuracy of precipitation reanalyses resulted in good river discharge simulations in a semi-arid basin. *Ecol. Eng.* **2019**, *131*, 107–119. [[CrossRef](#)]
25. Bitew, M.M.; Gebremichael, M. Evaluation of satellite rainfall products through hydrologic simulation in a fully distributed hydrologic model. *Water Resour. Res.* **2011**, *47*, 1–11. [[CrossRef](#)]
26. Lobligeois, F.; Andréassian, V.; Perrin, C.; Tabary, P.; Loumagne, C. When does higher spatial resolution rainfall information improve streamflow simulation? An evaluation using 3620 flood events. *Hydrol. Earth Syst. Sci.* **2014**, *18*, 575–594. [[CrossRef](#)]
27. Oliveira, V.A.; De Mello, C.R.; Beskow, S.; Viola, M.R.; Srinivasan, R. Modeling the effects of climate change on hydrology and sediment load in a headwater basin in the Brazilian Cerrado biome. *Ecol. Eng.* **2019**, *133*, 20–31. [[CrossRef](#)]
28. Silva, J.P.M.; da Silva, M.L.M.; da Silva, E.F.; da Silva, G.F.; de Mendonça, A.R.; Cabacinha, C.D.; Araújo, E.F.; Santos, J.S.; Vieira, G.C.; de Almeida, M.N.F.; et al. Computational techniques applied to volume and biomass estimation of trees in Brazilian savanna. *J. Environ. Manag.* **2019**, *249*, 109368. [[CrossRef](#)]

29. Nobrega, R.L.B.; Guzha, A.C.; Torres, G.N.; Kovacs, K.; Lamparter, G.; Amorim, R.S.S.; Couto, E.; Gerold, G. Identifying Hydrological Responses of Micro-Catchments under Contrasting Land Use in the Brazilian Cerrado. *Hydrol. Earth Syst. Sci. Discuss.* **2015**, *12*, 9915–9975. [CrossRef]
30. Myers, N.; Mittermeir, R.A.; Mittermeier, C.G.; Fonseca, G.A.B.; Kent, J. Biodiversity hotspots for conservation priorities. *Nature* **2000**, *403*, 853. [CrossRef]
31. Oliveira, P.T.S.; Nearing, M.A.; Moran, M.S.; Goodrich, D.C.; Wendland, E.; Gupta, H.V. Trends in water balance components across the Brazilian Cerrado. *Water Resour. Res.* **2014**, *50*, 7100–7114. [CrossRef]
32. Machado, A.R.; Wendland, E.; Krause, P. Hydrologic Simulation for Water Balance Improvement in an Outcrop Area of the Guarani Aquifer System. *Environ. Process.* **2016**, *3*, 19–38. [CrossRef]
33. Lima, J.E.F.W.; da Silva, E.M. Estimativa da contribuição hídrica superficial do Cerrado para as grandes regiões hidrográficas brasileiras. In *XVII Simpósio Brasileiro de Recursos Hídricos*; ABRH: São Paulo, Brazil, 2007; pp. 1–13.
34. Agência Nacional de Águas—ANA—Superintendência de Planejamento de Recursos Hídricos. Conjuntura Dos Recursos Hídricos no Brasil: Regiões Hidrográficas Brasileiras—Edição Especial 2015. Available online: <http://arquivos.ana.gov.br/institucional/sge/CEDOC/Catalogo/2015/ConjunturaDosRecursosHidricosNoBrasil2015.pdf> (accessed on 12 June 2019).
35. Xavier, A.C.; King, C.W.; Scanlon, B.R. Daily gridded meteorological variables in Brazil (1980–2013). *Int. J. Climatol.* **2016**, *36*, 2644–2659. [CrossRef]
36. Agência Nacional de Energia Elétrica (Brasil)—ANEEL Banco de Informações de Geração (BIG). Available online: <https://bit.ly/2IGf4Q0> (accessed on 12 June 2019).
37. Thiengo, S.C.; Santos, S.B.; Fernandez, M.A. Malacofauna límnic da área de influência do lago da usina hidrelétrica de Serra da Mesa, Goiás, Brasil. I. Estudo qualitativo. *Rev. Bras. Zool.* **2005**, *22*, 867–874. [CrossRef]
38. Alvares, C.A.; Stape, J.L.; Sentelhas, P.C.; De Moraes Gonçalves, J.L.; Sparovek, G. Köppen’s climate classification map for Brazil. *Meteorol. Z.* **2013**, *22*, 711–728. [CrossRef]
39. Hou, A.Y.; Kakar, R.K.; Neeck, S.; Azarbarzin, A.A.; Kummerow, C.D.; Kojima, M.; Oki, R.; Nakamura, K.; Iguchi, T. The Global Precipitation Measurement Mission. *Bull. Am. Meteorol. Soc.* **2014**, *95*, 701–722. [CrossRef]
40. Neitsch, S.L.; Arnold, J.G.; Kiniry, J.R.; Williams, J.R. *Soil and Water Assessment Tool Theoretical Documentation Version 2009*; Technical Report No.406; Texas Water Resources Institute: Forney, TX, USA, 2011.
41. Arnold, J.G.; Srinivasan, R.; Muttiah, R.S.; Williams, J.R. Large area hydrologic modeling and assessment part I: Model development. *J. Am. Water Resour. Assoc.* **1998**, *34*, 73–89. [CrossRef]
42. Arnold, J.G.; Moriasi, D.N.; Gassman, P.W.; Abbaspour, K.C.; White, M.J.; Srinivasan, R.; Santhi, C.; Harmel, R.D.; van Griensven, A.; Van Liew, M.W.; et al. SWAT: Model Use, Calibration, and Validation. *Trans. ASABE* **2012**, *55*, 1491–1508. [CrossRef]
43. PRIESTLEY, C.H.B.; TAYLOR, R.J. On the Assessment of Surface Heat Flux and Evaporation Using Large-Scale Parameters. *Mon. Weather Rev.* **1972**, *100*, 81–92. [CrossRef]
44. Hargreaves, G.H. Moisture Availability and Crop Production. *Trans. ASAE* **1975**, *18*, 0980–0984. [CrossRef]
45. Penman, H.L. Evaporation: An Introductory Survey. *Neth. J. Agric. Sci.* **1956**, *4*, 9–29. [CrossRef]
46. Monteith, J.L. Evaporation and environment. *Symp. Soc. Exp. Biol.* **1965**, 205–234.
47. Green, W.H.; Ampt, G.A. Studies on Soil Physics. *J. Agric. Sci.* **1911**, *4*, 1–24. [CrossRef]
48. United States Department of Agriculture—Soil Conservation Service (USDA-SCS) Section 4: Hydrology. In *National Engineering Handbook*; United States Department of Agriculture: Washington, DC, USA, 1972.
49. Neitsch, S.L.; Arnold, J.G.; Kiniry, J.R.; Williams, J.R. *Soil and Water Assessment Tool User’s Manual Version 2005*; Technical Report No. 406; Texas Water Resources Institute: Forney, TX, USA, 2005.
50. Srinivasan, R.; Ramanarayanan, T.S.; Arnold, J.G.; Bednarz, S.T. Large area hydrologic modeling and assessment part II: Model application. *J. Am. Water Resour. Assoc.* **1998**, *34*, 91–101. [CrossRef]
51. Empresa Brasileira de Pesquisa Agropecuária (EMBRAPA) Mapa de Solos do Brasil. Available online: http://geoinfo.cnps.embrapa.br/layers/geonode%3Asolos_br5m_2011_lat_long_wgs84 (accessed on 14 December 2019).
52. Instituto Brasileiro de Geografia e Estatística—IBGE Mudanças na Cobertura e Uso da Terra 2000. 2010–2012. Available online: http://maps.lapig.iesa.ufg.br/?layers=pa_br_uso_solo_500_ibge (accessed on 14 December 2019).

53. Abbaspour, K.C.; Yang, J.; Maximov, I.; Siber, R.; Bogner, K.; Mieleitner, J.; Zobrist, J.; Srinivasan, R. Modelling hydrology and water quality in the pre-alpine/alpine Thur watershed using SWAT. *J. Hydrol.* **2007**, *333*, 413–430. [[CrossRef](#)]
54. Guilhon, L.G.F.; Rocha, V.F.; Moreira, J.C. Comparação de Métodos de Previsão de Vazões Naturais Afluentes a Aproveitamentos Hidroelétricos. *Rev. Bras. Recur. Hídricos* **2007**, *12*, 13–20.
55. Oliveira, V.A.; de Mello, C.R.; Viola, M.R.; Srinivasan, R. Assessment of climate change impacts on streamflow and hydropower potential in the headwater region of the Grande river basin, Southeastern Brazil. *Int. J. Climatol.* **2017**, *37*, 5005–5023. [[CrossRef](#)]
56. Nóbrega, M.T.; Collischonn, W.; Tucci, C.E.M.; Paz, A.R. Uncertainty in climate change impacts on water resources in the Rio Grande Basin, Brazil. *Hydrol. Earth Syst. Sci.* **2011**, *15*, 585–595. [[CrossRef](#)]
57. Abbaspour, K.C. SWAT-CUP: SWAT Calibration and Uncertainty Programs—A User Manual 2015. Available online: https://swat.tamu.edu/media/114860/usermanual_swatcup.pdf (accessed on 14 December 2019).
58. Abbaspour, K.C.; Johnson, C.A.; van Genuchten, M.T. Estimating Uncertain Flow and Transport Parameters Using a Sequential Uncertainty Fitting Procedure. *Vadose Zone J.* **2004**, *3*, 1340–1352. [[CrossRef](#)]
59. Abbaspour, K.C.; Rouholahnejad, E.; Vaghefi, S.; Srinivasan, R.; Yang, H.; Kløve, B. A continental-scale hydrology and water quality model for Europe: Calibration and uncertainty of a high-resolution large-scale SWAT model. *J. Hydrol.* **2015**, *524*, 733–752. [[CrossRef](#)]
60. Triana, J.S.A.; Chu, M.L.; Guzman, J.A.; Moriasi, D.N.; Steiner, J.L. Beyond model metrics: The perils of calibrating hydrologic models. *J. Hydrol.* **2019**, *578*, 124032. [[CrossRef](#)]
61. Rodrigues, J.A.M.; Viola, M.R.; Alvarenga, L.A.; de Mello, C.R.; Chou, S.C.; de Oliveira, V.A.; Uddameri, V.; Morais, M.A.V. Climate change impacts under representative concentration pathway scenarios on streamflow and droughts of basins in the Brazilian Cerrado biome. *Int. J. Climatol.* **2019**, 1–16. [[CrossRef](#)]
62. Tan, M.; Samat, N.; Chan, N.; Roy, R. Hydro-Meteorological Assessment of Three GPM Satellite Precipitation Products in the Kelantan River Basin, Malaysia. *Remote Sens.* **2018**, *10*, 1011. [[CrossRef](#)]
63. Hosseini-Moghari, S.-M.; Tang, Q. Validation of GPM IMERG-V05 and V06 precipitation products over Iran. *J. Hydrometeorol.* **2020**. [[CrossRef](#)]
64. Wei, G.; Lü, H.; Crow, W.T.; Zhu, Y.; Wang, J.; Su, J. Evaluation of satellite-based precipitation products from IMERG V04A and V03D, CMORPH and TMPA with gauged rainfall in three climatologic zones in China. *Remote Sens.* **2018**, *10*, 30. [[CrossRef](#)]
65. Muhammad, E.; Muhammad, W.; Ahmad, I.; Muhammad Khan, N.; Chen, S. Satellite precipitation product: Applicability and accuracy evaluation in diverse region. *Sci. China Technol. Sci.* **2020**. [[CrossRef](#)]
66. Kling, H.; Fuchs, M.; Paulin, M. Runoff conditions in the upper Danube basin under an ensemble of climate change scenarios. *J. Hydrol.* **2012**, *424–425*, 264–277. [[CrossRef](#)]
67. Moriasi, D.N.; Arnold, J.G.; Van Liew, M.W.; Bingner, R.L.; Harmel, R.D.; Veith, T.L. Model Evaluation Guidelines for Systematic Quantification of Accuracy in Watershed Simulations. *Trans. ASABE* **2007**, *50*, 885–900. [[CrossRef](#)]
68. Zad, S.N.M.; Zulkafli, Z.; Muharram, F.M. Satellite rainfall (TRMM 3B42-V7) performance assessment and adjustment over Pahang river basin, Malaysia. *Remote Sens.* **2018**, *10*, 388. [[CrossRef](#)]
69. Su, J.; Haishen, L.; Ryu, D.; Zhu, Y. The Assessment and Comparison of TMPA and IMERG Products Over the Major Basins of Mainland China. *Earth Space Sci.* **2019**, *6*, 2461–2479. [[CrossRef](#)]
70. Rozante, J.R.; Vila, D.A.; Chiquetto, J.B.; de Fernandes, A.A.; Alvim, D.S. Evaluation of TRMM/GPM blended daily products over Brazil. *Remote Sens.* **2018**, *10*, 882. [[CrossRef](#)]
71. Varma, A.K.; Varma, A.K.B. Measurement of Precipitation from Satellite Radiometers (Visible, Infrared, and Microwave): Physical Basis, Methods, and Limitations. In *Remote Sensing of Aerosols, Clouds, and Precipitation*; Islam, T., Hu, Y., Kokhanovsky, A., Wang, J., Eds.; Elsevier: Iowa City, IA, USA, 2018; pp. 223–248. ISBN 9780128104385.
72. Jiang, S.; Ren, L.; Xu, C.Y.; Yong, B.; Yuan, F.; Liu, Y.; Yang, X.; Zeng, X. Statistical and hydrological evaluation of the latest Integrated Multi-satellite Retrievals for GPM (IMERG) over a midlatitude humid basin in South China. *Atmos. Res.* **2018**, *214*, 418–429. [[CrossRef](#)]
73. Correa, S.W.; de Paiva, R.C.D.; Siqueira, V.; Collischonn, W.; Paiva, R.C.D.; Siqueira, V.; Collischonn, W. Hydrological reanalysis across the 20th century: A case study of the Amazon Basin. *J. Hydrol.* **2019**, *570*, 755–773. [[CrossRef](#)]

74. Zhu, H.; Li, Y.; Huang, Y.; Li, Y.; Hou, C.; Shi, X. Evaluation and hydrological application of satellite-based precipitation datasets in driving hydrological models over the Huifa river basin in Northeast China. *Atmos. Res.* **2018**, *207*, 28–41. [[CrossRef](#)]
75. Li, D.; Christakos, G.; Ding, X.; Wu, J. Adequacy of TRMM satellite rainfall data in driving the SWAT modeling of Tiaoxi catchment (Taihu lake basin, China). *J. Hydrol.* **2018**, *556*, 1139–1152. [[CrossRef](#)]
76. Da Silva, R.M.; Dantas, J.C.; de Beltrão, J.A.; Santos, C.A.G. Hydrological simulation in a tropical humid basin in the cerrado biome using the SWAT model. *Hydrol. Res.* **2018**, *49*, 908–923. [[CrossRef](#)]
77. Junqueira, R.; Viola, M.R.; de Mello, C.R.; Vieira-Filho, M.; Alves, M.V.G.; da Amorim, J.S. Drought severity indexes for the Tocantins River Basin, Brazil. *Theor. Appl. Climatol.* **2020**, *141*, 465–481. [[CrossRef](#)]
78. Nerini, D.; Zulkafli, Z.; Wang, L.P.; Onof, C.; Buytaert, W.; Lavado-Casimiro, W.; Guyot, J.L. A comparative analysis of TRMM–rain gauge data merging techniques at the daily time scale for distributed rainfall–runoff modeling applications. *J. Hydrometeorol.* **2015**, *16*, 2153–2168. [[CrossRef](#)]



© 2020 by the authors. Licensee MDPI, Basel, Switzerland. This article is an open access article distributed under the terms and conditions of the Creative Commons Attribution (CC BY) license (<http://creativecommons.org/licenses/by/4.0/>).